31st Annual International Conference of the IEEE EMBS
Minneapolis, Minnesota, USA, September 2-6, 2009

Numerical Analysis of a Comprehensive *In Silico* Subcutaneous Insulin Absorption Compartmental Model

Daniel Sebald and Timothy Ruchti

Abstract— **Development of safe and effective glucose management algorithms for remediation of inpatient hyperglycemia reduces nursing workload and improves patient outcomes by providing decision support at the bedside. Computer simulation of drug pharmacokinetics and pharmacodynamics enables evaluation and testing of glycemic control algorithms prior to *in vivo* investigations without risk to patients. For subcutaneous insulin dosing, *in silico* testing requires an accurate model of diffusion and availability of insulin from the time of injection. Wong *et al.* [1, 2] have recently proposed a comprehensive compartmental model of pharmacokinetics for six types of insulin to serve as the basis for available brands. The compartmental model is efficient for processing a large number of virtual patients. Herein we analyze numerical integration properties for the Wong *et al.* model, as a guide for achieving peak efficiency of simulations.**

I. Introduction

With the emergence of bedside devices in hospital ICUs and wards comes the opportunity to integrate decision support (DS) utilities on computers and smart infusion pumps to assist nurses and clinicians in providing an alternative to paper-based protocols. One approach to DS is to transfer existing paper-based protocols–of which there are many–to computer for automation. Another approach is to develop new therapeutic algorithms that may be too complex for paper calculation, but provide improved personalization through adaptive control.

In silico, or computer-simulation-based, testing offers a safe means to develop and compare dosing control algorithms outside the hospital setting prior to clinical testing. Simulation requires two components aside from the DS control strategy: a large database of virtual patients and a pharmacokinetic/pharmacodynamic (PKPD) model, both representing the cohort. In choosing a PKPD model, the researcher must strike a balance between one which accurately reflects the underlying physiology, *e.g.*, the endocrine system, and one which is efficient enough to conduct large *in silico* trials within a reasonable time frame.

In the case of blood glucose management for Type-I, Type-II and stress-induced diabetic patients the trend in the simulation community, as surveyed by Nucci and Cobelli [3], has been toward an efficient compartmental model where physiological system components such as plasma glucose concentration and subcutaneous injection volume are associated with variables in a system of ordinary differential equations (ODE). In [1], Wong *et al.* have constructed an extensive and comprehensive ten-compartment model for the pharmacokinetics of absorption for rapid-acting, regular and long-acting insulin after extensively searching past literature for pertinent models and parameters. The authors then verify the model in [2].

Here we analyze the underlying dynamical structure in terms of numerical integration for the Wong *et al.* ten-compartment pharmacokinetic model representing the following six types of insulin administered subcutaneously: monomeric, regular, neutral protamine Hagedorn (NPH), lente, ultralente and glargine. The absorption model serves a role in a larger PKPD system exhibiting further dynamic behavior requiring more numerical analysis for optimizing efficiency, but the injection kinetics serve merely as input and there are no inter-relationships of system components that might alter the absorption subsystem eigen-structure. Another element of this paper is to rate some common ODE solvers applied to absorption simulation.

D. Sebald (daniel.sebald@hospira.com) and T. Ruchti are with the Global Device R&D department of Hospira, Inc., Lake Forest, IL.

II. Subcutaneous Absorption Model of [1, 2]

A. Compartmental Model

The Wong *et al.* model has ten compartments (see Fig. 1 in [1] for an illustration), which we arrange into vector

$$\mathbf{x}(t) = \begin{bmatrix} I(t) \\ x_i(t) \\ x_{\text{dm}}(t) \\ x_{\text{h}}(t) \\ c_{\text{NPH}}(t) \\ c_{\text{len}}(t) \\ x_{\text{h,ulen}}(t) \\ c_{\text{ulen}}(t) \\ x_{\text{h,gla}}(t) \\ p_{\text{gla}}(t) \end{bmatrix} \tag{1}$$

where $I(t)$ is plasma insulin concentration (mU/liter), and remaining variables are mass in the $x_i(t)$ interstitium compartment (mU), $x_{\text{h}}(t)$ hexameric compartment (mU), $x_{\text{dm}}(t)$ dimer/monomer compartment (mU), $c_{\text{NPH}}(t)$ NPH crystalline protamine compartment (mU), $c_{\text{len}}(t)$ lente crystalline zinc compartment (mU), $x_{\text{h,ulen}}(t)$ ultralente hexameric compartment (mU), $c_{\text{ulen}}(t)$ ultralente crystalline zinc compartment (mU), $x_{\text{h,gla}}(t)$ glargine hexameric compartment (mU), and $p_{\text{gla}}(t)$ glargine precipitate compartment (mU). The plasma insulin concentration $I(t)$ serves as the input to the pharmacodynamic model of the endocrine system.

All but the last two model equations in $\mathbf{x}(t)$ are linear, enabling compact notation similar to a conventional linear system of ODEs. The authors of [1, 2] approximate the maximum rate of dissolution for glargine amorphous micro-precipitate to hexameric form as

$$r_{\text{dis,max}}(t_i \leq t < t_{i+1}) = \begin{cases} 15\,, & \text{if } u_{\text{p,gla}}(t_i) < 30,000 \\ 15\left(\frac{u_{\text{p,gla}}(t_i)}{30,000}\right), & \text{if } u_{\text{p,gla}}(t_i) \geq 30,000 \end{cases} \tag{2}$$

where $u_{\text{p,gla}}(t)$ is the subcutaneous injection rate for the precipitate fraction of glargine and t_i is time of injection. For convenience, define $\Omega = \{t : r_{\text{dis,max}}(t) < k_{\text{prec,gla}} x_{10}(t)\}$, where $k_{\text{prec,gla}}$ is the decay constant for the precipitate compartment, and define $1_\Omega(t)$ the indicator function of set Ω. Then

$$\mathbf{x}'(t) = \mathbf{A}_i \mathbf{x}(t) + \begin{bmatrix} \mathbf{0}_{8\times 1} \\ (r_{\text{dis,max}}(t) - k_{\text{prec,gla}} x_{10}(t)) \\ -(r_{\text{dis,max}}(t) - k_{\text{prec,gla}} x_{10}(t)) \end{bmatrix} 1_\Omega(t) + \mathbf{B}\mathbf{u}(t) \tag{3}$$

where elements of vector $\mathbf{x}(t) \in \mathbb{R}^{10}$ represent the compartments of the model, $\mathbf{A}_i \in \mathbb{R}^{10} \times \mathbb{R}^{10}$ is a coefficient matrix, $\mathbf{u}(t) \in \mathbb{R}^{18}$

978-1-4244-3296-7/09/$25.00 ©2009 IEEE

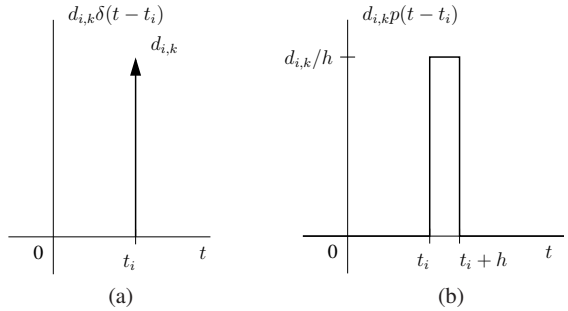

Fig. 1. Each injection is modeled as (a) a shifted unit impulse or (b) a shifted unit pulse $p(t-t_i)$ multiplied by dosage $d_{i,k}$.

represents the insulin input (explained later), and $\mathbf{B} \in \mathbb{R}^{10} \times \mathbb{R}^{18}$ is a coefficient matrix.

Sparse matrix $\mathbf{A}_i$ is upper diagonal and appears in Fig. 2. In brief, one can think of the parameters as the decay or disassociation constants for the compartments associated with the variables in (1). For a detailed description of all parameters see [1]. The rate of diffusion loss, coefficient k_d, is actually a function of the injected insulin volume V_{inj}. Thus $\mathbf{A}_i$ is technically time-varying, and we deal with this on a piece-wise constant basis for each injection i.

B. Input Model

Wong *et al.* use a simplification of the hexameric/dimeric equilibrium dynamics developed in [4, 5]. Aside from the monomeric insulin, the remaining types of insulin, when injected, are distributed according to the three equations

$$u_{\text{p/c}}(t) = \alpha\, u_{\text{total}}(t) \tag{5}$$

$$u_{\text{h}}(t) + u_{\text{dm}}(t) = (1-\alpha)\, u_{\text{total}}(t) \tag{6}$$

$$\frac{u_{\text{h}}(t_i)}{V_{\text{inj},i}} = Q_{\text{D}} \left(\frac{u_{\text{dm}}(t_i)}{V_{\text{inj},i}} \right)^3 \tag{7}$$

where Q_{D} (ml/mU)^2 is an hexameric-dimeric equilibrium constant and $V_{\text{inj},i}$ (ml) is volume of injection i. The implicit solution of (5)–(7) follows from choosing the real root of polynomial

$$\frac{Q_{\text{D}}}{V_{\text{inj},i}^3} u_{\text{dm}}^3(t_i) + 0 + \frac{1}{V_{\text{inj},i}} u_{\text{dm}}(t_i) - \frac{(1-\alpha) u_{\text{total}}(t_i)}{V_{\text{inj},i}} = 0. \tag{8}$$

The dosage vector for an injection is formed by arranging elements according to the six brand types (monomeric, regular, NPH, lente, ultralente and glargine) and subdividing by the three equilibrium types (monomeric/dimeric, hexameric and crystalline/precipitate). Figs. 3 and 4 show the appropriate sparse input matrix and dosage vector to achieve the model equations in [1].

We consider two methods of putting insulin injection doses into the PKPD simulation. The first is an instantaneous appearance of insulin modeled by a scaled and shifted Dirac delta function, $\mathbf{d}_i \delta(t-t_i)$, as illustrated in Fig. 1a. This is achieved by running simulations in piece-wise intervals and adding $\mathbf{B}\mathbf{d}_i$ to the final state of an interval to serve as the initial value of the next interval. A second method of incorporating injections is to spread the dosage across the smallest interval of interest, h, as illustrated in Fig. 1b, where

$$p(t) = \begin{cases} 1/h, & 0 \le t < h \\ 0, & \text{otherwise} \end{cases} \tag{9}$$

i.e., $\mathbf{d}_i p(t-t_i)$. Note that h is not necessarily the same as the interval of numerical integration, ϵ, in the case of adaptive step-size methods. The appendix describes the second method's integral.

III. Numerical Integration

Generally, nonlinear ODEs are numerically integrated using a solver, and there are several ways one could approach introducing subcutaneous insulin injections into simulation, summarized as follows:

1) adaptive step-size w/ instantaneous or distributed injection
2) fixed step-size w/ distributed injection (AVOID)
3) fixed step-size w/ instantaneous injection.

Adaptive step-size ODE solvers implement two similar solvers of differing order in parallel, estimating the integration error per step and retrying with smaller step size when the error is out of tolerance. For example, MATLAB routine `ode45` is a Runge-Kutta (RK) 4th order algorithm in combination with an RK 5th order algorithm for estimating truncation errors. The approach has the advantage of decreasing the integration interval around difficult areas, such as with the discontinuities of the distributed injection model of Fig. 1b. (See [6] for an example of decreasing step size near discontinuity.) At the same time the adaptive approach increases the integration interval when possible, thus achieving efficiency.

In a similar vein, using a fixed integration step size, ϵ, and injections modeled as distributed pulses is fraught with large error if ϵ is the same as the interval of interest, h, or with poor efficiency if ϵ is taken as a fraction of h.

The third approach—piece-wise integration between injections with $\mathbf{B}\mathbf{d}_i$ added to the final value of interval $i-1$ as the initial value of interval i—does not suffer from inaccurate integration of the input. We will analyze this approach as a means of illustrating numerical properties.

An ODE of the exponential variety, such as (3) is potentially stiff, and the eigenvalues of its Jacobian matrix provide a stiffness index [7]. That is, provided $Re(\lambda_i) < 0$ for all i,

$$L = \max |Re(\lambda_i)| \tag{11}$$

and if $Lh \gg 1$, where h is the length of an interval of interest, the system is stiff on the interval in question.

Furthermore, the stability of the numerical technique in combination with system dynamics must be ensured. Consider a fixed step-size solver such as MATLAB routine `ode4`, an implementation of the well-known RK 4th order algorithm.[1] The stability function for Runge-Kutta methods is

$$\phi(z) = \frac{\det(\mathbf{I} - z\mathbf{T} + z\mathbf{e}\mathbf{v}^T)}{\det(\mathbf{I} - z\mathbf{T})} \tag{12}$$

where $\mathbf{T}$ and $\mathbf{v}$ come from the associated Butcher tableau and $\mathbf{e}$ is a vector of ones. With each injection, one can verify the eigenvalues of the Jacobian matrix (in the case of (3), simply $\mathbf{A}_i$) and integration step size satisfy

$$|\phi(h\lambda_i)| < 1.0 \tag{13}$$

Fig. 5 shows the profile of 10 U of insulin, for all six varieties, injected at time zero when using the median model parameters from Table 9 in [1]. The key for Fig. 5 lists insulin types in order of largest to smallest peak concentration. Eigenvalues of the corresponding Jacobian matrix $\mathbf{A}_i$ range from –0.0008 to –0.16; all negative as expected. By criteria (11), stiffness problems should arise for $h \approx 6.25$ min and greater.

To test the above hypothesis, consider the results of simulations varying h logarithmically in the range 0.2 to 20 min for monomeric insulin. At each integration interval, Fig. 6 shows $\phi(\lambda_{\max} h)$ where the stability criteria is met up until $h = 10$ min. Thus we expect

[1] http://www.mathworks.com/support/tech-notes/1500/1510.html#fixed.

$$\mathbf{A}_i = \begin{bmatrix} -n & k_3/(V_{\mathrm{i}}\, m_{\mathrm{b}}) & 0 & 0 & 0 & 0 & 0 & 0 & 0 & 0 \\ 0 & -(k_3 + k_{\mathrm{d,i}}) & k_2 & 0 & 0 & 0 & 0 & 0 & 0 & 0 \\ 0 & 0 & -(k_2 + k_{\mathrm{d}}) & k_1 & 0 & 0 & k_{1,\mathrm{ulen}} & 0 & k_{1,\mathrm{gla}} & 0 \\ 0 & 0 & 0 & -(k_1 + k_{\mathrm{d}}) & k_{\mathrm{crys,NPH}} & k_{\mathrm{crys,len}} & 0 & 0 & 0 & 0 \\ 0 & 0 & 0 & 0 & -k_{\mathrm{crys,NPH}} & 0 & 0 & 0 & 0 & 0 \\ 0 & 0 & 0 & 0 & 0 & -k_{\mathrm{crys,len}} & 0 & 0 & 0 & 0 \\ 0 & 0 & 0 & 0 & 0 & 0 & -(k_{1,\mathrm{ulen}} + k_{\mathrm{d}}) & k_{\mathrm{crys,ulen}} & 0 & 0 \\ 0 & 0 & 0 & 0 & 0 & 0 & 0 & -k_{\mathrm{crys,ulen}} & 0 & 0 \\ 0 & 0 & 0 & 0 & 0 & 0 & 0 & 0 & -(k_{1,\mathrm{gla}} + k_{\mathrm{d}}) & k_{\mathrm{prec,gla}} \\ 0 & 0 & 0 & 0 & 0 & 0 & 0 & 0 & 0 & -k_{\mathrm{prec,gla}} \end{bmatrix} \tag{4}$$

Fig. 2. Sparse system matrix.

$$\mathbf{B} = \begin{bmatrix} 0&0&0&0&0&0&0&0&0&0&0&0&0&0&0&0&0&0 \\ 0&0&0&0&0&0&0&0&0&0&0&0&0&0&0&0&0&0 \\ 1&0&0&1&0&0&1&0&0&1&0&0&1&0&0&1&0&0 \\ 0&0&0&0&1&0&0&1&0&0&1&0&0&0&0&0&0&0 \\ 0&0&0&0&0&0&0&0&1&0&0&0&0&0&0&0&0&0 \\ 0&0&0&0&0&0&0&0&0&0&0&1&0&0&0&0&0&0 \\ 0&0&0&0&0&0&0&0&0&0&0&0&0&1&0&0&0&0 \\ 0&0&0&0&0&0&0&0&0&0&0&0&0&0&1&0&0&0 \\ 0&0&0&0&0&0&0&0&0&0&0&0&0&0&0&1&0&0 \\ 0&0&0&0&0&0&0&0&0&0&0&0&0&0&0&0&1&0 \\ 0&0&0&0&0&0&0&0&0&0&0&0&0&0&0&0&0&1 \end{bmatrix} \tag{10}$$

Fig. 3. Sparse input matrix.

and do find divergence problems for $h \geq 10$ min in error plots in Fig. 7 and Fig. 8, where the dashed line represents 0.1%. The error plots show $|I_{\mathrm{sim}}(t) - I_{\mathrm{lin}}(t)|/I_{\mathrm{lin}}(t)$, where $I_{\mathrm{lin}}(t)$ is the closed-form solution of the linear system, which is $\exp(\mathbf{A}_i(t-t_i))\mathbf{B}\mathbf{d}_i$ for injection model Fig. 1a and (18) in the appendix for injection model Fig. 1b. Simulations for $h = 12.4$ and 15.7 min show marginal instability, while trial $h = 20$ min exhibits extreme divergence.

Figure 7 shows relative error at peak plasma insulin concentration. Accuracy at the concentration peak is quite good until approximately $h = 5$ min, where the monomeric insulin simulation shows erratic behavior. Being the shortest acting insulin model, monomeric absorption is associated with the fastest decaying mode, *i.e.*, the largest magnitude eigenvalue, and is the most susceptible to stiffness and convergence problems.

Figure 8 shows the maximum relative absolute insulin concentration error across the whole simulation interval, not just peak. Errors associated with concentration values less than 2% of the peak concentration were discarded. (The error is not of interest when the concentration is at levels on order of the noise in the system.) The shift of error curves to the left in Fig. 8 compared to Figure 7 indicate that the largest error does not occur at the peak.

IV. Conclusions

Numerical analysis applied to the Wong *et al.* subcutaneous insulin absorption model indicates that a fixed integration interval of approximately five minutes or less will provide good accuracy for simulating insulin absorption. The larger PKPD system in which the model is used requires similar analysis. The suggested methodology for efficient simulation is to use an adaptive ODE solver, setting its maximum interval of integration to near the stable and non-stiff limits suggested by analysis, *e.g.*, in this case one to five minutes.

Table I shows accuracy for several ODE solvers applied to NPH insulin injections. The adaptive ODE solver will allow injections to

$$\mathbf{d}_i = \begin{bmatrix} u_{\mathrm{mono}}(t_i) \\ 0 \\ 0 \\ u_{\mathrm{m,RH}}(t_i) \\ u_{\mathrm{h,RH}}(t_i) \\ 0 \\ u_{\mathrm{m,NHP}}(t_i) \\ u_{\mathrm{h,NPH}}(t_i) \\ u_{\mathrm{c,NPH}}(t_i) \\ u_{\mathrm{m,len}}(t_i) \\ u_{\mathrm{h,len}}(t_i) \\ u_{\mathrm{c,len}}(t_i) \\ u_{\mathrm{m,ulen}}(t_i) \\ u_{\mathrm{h,ulen}}(t_i) \\ u_{\mathrm{c,ulen}}(t_i) \\ u_{\mathrm{m,gla}}(t_i) \\ u_{\mathrm{h,gla}}(t_i) \\ u_{\mathrm{p,gla}}(t_i) \end{bmatrix} \tag{14}$$

Fig. 4. Injection dose vector at time t_i.

be modeled as an instantaneous or distributed across the minimum interval of interest. The fixed step-size algorithm is suitable for injections modeled as instantaneous impulse, but performs poorly for the distributed pulse scenario. Generally, ODE solvers designed for stiff problems perform marginally better for the subcutaneous insulin absorption PK model.

Appendix

The solution to linear, constant coefficient ODE

$$\mathbf{x}'(t) = \mathbf{A}\mathbf{x}(t) + \mathbf{B}\mathbf{u}(t) \tag{15}$$

is [8]

$$\mathbf{x}(t) = e^{\mathbf{A}(t-t_0)}\mathbf{x}_0 + \int_{t_0}^{t} e^{\mathbf{A}(t-\tau)}\mathbf{B}\mathbf{u}(\tau)\,\mathrm{d}\tau \tag{16}$$

where the last term is commonly known as the convolution integral and $e^{\mathbf{A}t}$ as the system impulse response. Let $\mathbf{d}_i$ be a dose vector. Then $\mathbf{u}(t) = \sum_i \mathbf{d}_i p(t - t_i)$. For sake of simplicity, we drop the summation and focus on a single injection at, say, time t_i. Through use of similarity transformation $\mathbf{A}_i = \mathbf{Q}_i\mathbf{D}_i\mathbf{Q}_i^{-1}$, where $\mathbf{D}_i$ is a diagonal matrix of eigenvalues (or more generally, in Jordon canonical form), (16) becomes

$$\begin{aligned} \mathbf{x}(t) &= e^{\mathbf{A}_i(t-t_i)}\mathbf{x}_i + \int_{t_i}^{t} e^{\mathbf{A}_i(t-\tau)}\mathbf{B}\mathbf{d}_i p(\tau)\,\mathrm{d}\tau \\ &= e^{\mathbf{A}_i(t-t_i)}\mathbf{x}_i + \left(\int_{t_i}^{t} e^{\mathbf{A}_i(t-\tau)} p(\tau)\,\mathrm{d}\tau\right)\mathbf{B}\mathbf{d}_i \end{aligned}$$

TABLE I

ACCURACY OF NPH PHARMACOKINETIC SIMULATION WITH FIXED INTEGRATION INTERVAL (NON-ADAPTIVE) OR MAXIMUM/INITIAL INTEGRATION INTERVAL (ADAPTIVE) SET TO FIVE MINUTES FOR VARIOUS TECHNIQUES; LISTED FROM BEST TO WORST.

Program	Solver	Type	Application	max rel abs err, NPH		†CPU time (s)	Quality
				impulse	pulse		
Octave	odebda	MEBDF	stiff	3.01 e -5	8.82 e -5	0.720	exceptional
MATLAB	ode23s	RK	stiff	7.84 e -4	5.28 e -4	0.250	exceptional
MATLAB	ode45	RK	non-stiff	3.96 e -5	1.11 e -3	0.109	good
Octave	ode45	RK	non-stiff	2.23 e -4	6.40 e -5	0.788	good
MATLAB	‡ode4	RK	–	6.64 e -6	3.34 e -2	0.219	limited
Octave	ode23	RK	non-stiff	1.63 e -2	1.67 e -1	0.488	very limited

†Octave and MATLAB run on different computers.
‡Non-adaptive solver uses five times oversampling.

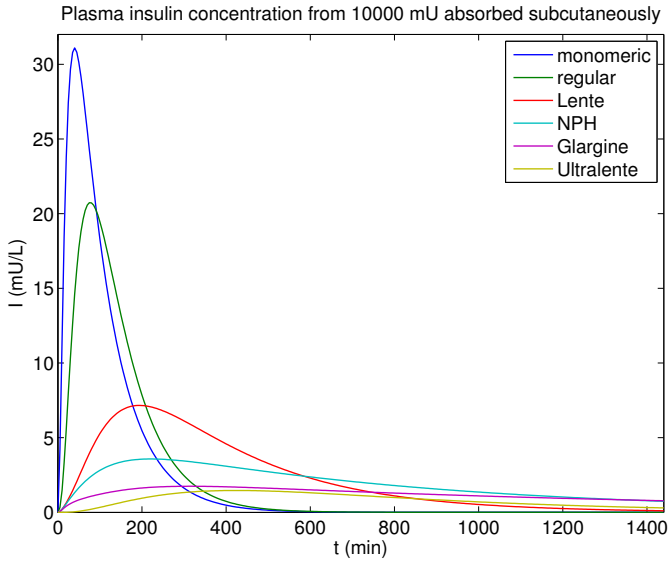

Fig. 5. Pharmacokinetic absorption curves for the six types of insulin included in the Wong *et al.* model [1].

$$= e^{\mathbf{A}_i(t-t_i)}\mathbf{x}_i + \left(\int_{t_i}^{t} \mathbf{Q}_i e^{\mathbf{D}_i(t-\tau)}\mathbf{Q}_i^{-1} p(\tau)\,\mathrm{d}\tau\right)\mathbf{B}\mathbf{d}_i$$
$$= e^{\mathbf{A}_i(t-t_i)}\mathbf{x}_i + \mathbf{Q}_i\left(\int_{t_i}^{t} e^{\mathbf{D}_i(t-\tau)} p(\tau)\,\mathrm{d}\tau\right)\mathbf{Q}_i^{-1}\mathbf{B}\mathbf{d}_i. \quad (17)$$

Applying integral (17) for a pulse lasting h minutes gives

$$\mathbf{x}(t) = \begin{cases} \mathbf{0}, & t \le t_i \\ e^{\mathbf{A}_i(t-t_i)}\mathbf{x}_i + \frac{1}{h}\mathbf{Q}_i\mathbf{D}_i^{-1}\left[e^{\mathbf{D}_i(t-t_i)} - \mathbf{I}\right]\mathbf{Q}_i^{-1}\mathbf{B}\mathbf{d}_i, & t_i < t \le t_i + h \\ e^{\mathbf{A}_i(t-t_i)}\mathbf{x}_i + \frac{1}{h}\mathbf{Q}_i\mathbf{D}_i^{-1}e^{\mathbf{D}_i(t-t_i)}\left[\mathbf{I} - e^{-h\mathbf{D}_i}\right]\mathbf{Q}_i^{-1}\mathbf{B}\mathbf{d}_i, & t > t_i + h. \end{cases} \quad (18)$$

REFERENCES

[1] J. Wong, J. G. Chase, C. E. Hann, G. M. Shaw, T. F. Lotz, J. Lin, and A. J. Le Compte, "A subcutaneous insulin pharmacokinetic model for computer simulation in a diabetes decision support role: Model structure and parameter identification," *J. Diabetes Sci. Tech.*, vol. 2, no. 4, pp. 658–671, July 2008.

[2] ——, "A subcutaneous insulin pharmacokinetic model for computer simulation in a diabetes decision support role: Validation and simulation," *J. Diabetes Sci. Tech.*, vol. 2, no. 4, pp. 672–680, July 2008.

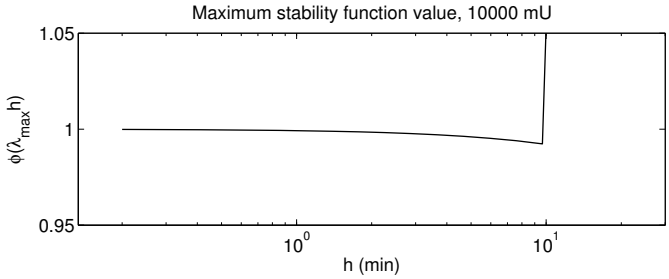

Fig. 6. Stability function values.

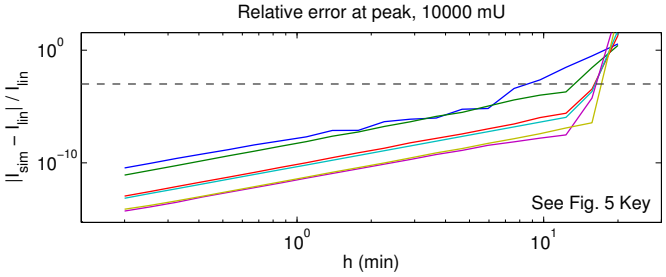

Fig. 7. Relative error at peak plasma insulin concentration.

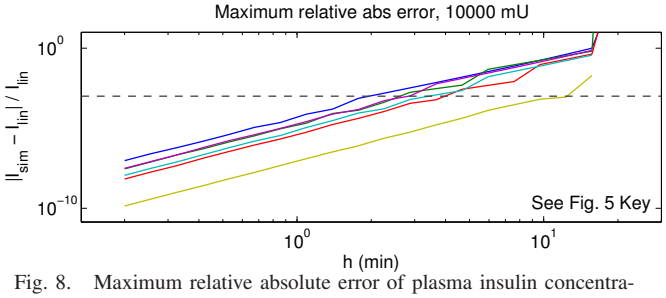

Fig. 8. Maximum relative absolute error of plasma insulin concentration.

[3] G. Nucci and C. Cobelli, "Models of subcutaneous insulin kinetics. A critical review," *Comp. Methods Prog. Biomed.*, vol. 62, pp. 249–257, July 2000.

[4] E. Mosekilde, K. S. Jensen, C. Binder, S. Pramming, and B. Thorsteinsson, "Modeling absorption kinetics of subcutaneous injected soluble insulin," *J. Pharmacokin. Biopharm.*, vol. 17, no. 1, pp. 67–87, 1989.

[5] T. Søeborg, C. H. Rasmussen, E. Mosekilde, and M. Colding-Jørgensen, "Absorption kinetics of insulin after subcutaneous administration," *Euro. J. Pharmaceut. Sci.*, vol. 17, no. 1, pp. 67–87, 2009.

[6] B. T. Kulakowski, , J. F. Gardner, and J. L. Shearer, *Dynamic modeling and control of engineering systems*. New York: Cambridge, 2007.

[7] L. F. Shampine, *Numerical Solution of Ordinary Differential Equations*. New York: Chapman & Hall, 1994.

[8] C.-T. Chen, *Linear system theory and design*. New York: Harcourt Brace Jovanovich, 1984.